Eur. J. Mech. B - Fluids 20 (2001) 799–812

S0997-7546(01)01139-6/FLA

Response of the boundary layer developing over a blunt-nosed flat plate to free-stream non-uniformities

Maxim V. Ustinov

Central Aerohydrodynamics Institute (TsAGI), Zhukovsky-3, 140180, Russia

(Received 17 December 1999; revised 1 March 2001; accepted 24 March 2001)

Abstract – The response of the boundary layer on a flat plate with blunt nose to infinitesimally small non-uniformity in the freestream velocity along the span has been studied. The non-uniformity was shown to excite boundary-layer disturbances similar to streaks or Klebanoff modes generally observed in experiments conducted with a high level of free-stream turbulence. The boundary layer disturbances have a predominantly streamwise velocity component and exhibit transient growth. In contrast to streaks generated by streamwise vortices impinging on the sharp nose of a plate, the disturbances produced by free-stream non-uniformity interaction with a blunt nose have a different level of growth. Their maximal amplification scales with the Reynolds number, based on the size of nose bluntness and is almost independent of the spanwise period of disturbances. This difference was shown to be caused by additional amplification of disturbances via vortex lines stretching around the leading edge. © 2001 Éditions scientifiques et médicales Elsevier SAS

boundary layer / receptivity / vorticity / transition

Nomenclature

Dimensional variables

x', y', z'	streamwise, spanwise and vertical coordinates, m
b'	size of leading edge bluntness, m
λ'	spanwise period of flow non-uniformity, m
d'	width of localized flow non-uniformity, m
r'	radius of leading edge, m
δ'	boundary layer thickness, m
u_∞	outer flow velocity, ms^{-1}
ρ	density of fluid, kgm^{-3}
ν	kinematic viscosity, $\mathrm{m}^2\mathrm{s}^{-1}$
σ	damping coefficient of non-uniformity in free stream, m^{-1}
x'_m	streamwise location of maximum of disturbances, m
λ'_m	spanwise period of disturbance which gives maximum amplification at fixed downstream position, m
u'_m	maximal over y', z' disturbance of streamwise velocity, ms^{-1}

E-mail address: ustinov@stb.aerocentr.msk.su (M.V. Ustinov).

Non-dimensional variables

ε	amplitude of non-uniformity
U_b, W_b	streamwise and vertical velocity components in undisturbed flow around the plate
u, v, w	streamwise, spanwise and vertical velocity components of disturbance
p	disturbance of pressure
a	constant related with local velocity gradient in the vicinity of leading edge
R	Reynolds number based on spanwise period of non-uniformity
R_b, R_r, R_x	Reynolds numbers based on size of leading edge bluntness, radius of leading edge and streamwise coordinate respectively
A	amplification coefficient of disturbance at leading edge
$X, y, Z,$	non-dimensional streamwise, spanwise and vertical coordinates
U, V, W	normalized streamwise, spanwise and vertical velocity components of disturbances for sinusoidal oncoming non-uniformity
P	normalized disturbance of pressure
U_m	maximal in Z value of normalized disturbance of streamwise velocity
U_0, W_0	streamwise and vertical velocity components in Blasius boundary layer
$\eta = Z/\sqrt{X}$	boundary layer coordinate
f	function describing self-similar solution for Blasius boundary layer
W_{00}	vertical velocity at the outer edge of boundary layer
X_0	location of initial section for numerical solution
$Z_{\max}$	outer boundary of computational domain
u_m	maximal disturbance of streamwise velocity
$g(y)$	spanwise profile of localized flow non-uniformity
$F(\beta)$	Fourier transform of $g(y)$
β	Fourier variable

overbar $\overline{\dots}$ denotes the non-dimensional variables and normalized disturbance for localized flow non-uniformity

1. Introduction

Longitudinal streaky structures or Klebanoff modes usually appear in boundary layers subjected to free-stream turbulence [1–3]. These structures are believed to give rise to the so-called by-pass transition (term introduced by Morkovin [4]). Present consensus is that streaks are generated by low-frequency vortical disturbances in the oncoming flow. Because of this, boundary layer receptivity to steady or quasi-steady free-stream vorticity has been intensively studied. Most of the works deal with streamwise vortices interacting with a boundary layer [5–8]. Having cross-flow velocity, these disturbances exhibit transient growth in the boundary layer and are transformed into alternating low and high velocity streaks. Computations using the PSE-method developed by Herbert and Lin [5] and Bertolotti [6] showed a good agreement of the resulting boundary layer distortion with streaky structures observed in experiments. The upstream perturbations that maximize the spatial energy growth (called ‘optimal disturbances’) were found by Andersson et al. [7], Luchini [8] for

boundary layer flow and by Reshotko and Tumin [9] for flow in a circular pipe. The optimal disturbances correspond to streamwise vortices and the downstream response corresponds to streamwise streaks.

However, experiments by Bradshaw [10], Watmuff [11], Kachanov et al. [12], Sboev et al. [13] revealed that flow non-uniformity along the span or free-stream vorticity normal to a leading edge produces streaks as well as streamwise vortices. Assuming that flow non-uniformity is accompanied by slight steady spanwise velocity modulated along the span, Crow [14] found resulting boundary layer distortion. His results well describe the vertical profiles of velocity pulsations in boundary layer measured in experiments [1,2,10]. The appearance of cross flow, when a uni-directional nonuniform flow interacts with the leading edge, was explained in the work of Goldstein et al. [15]. The flow non-uniformity is associated with vertical vorticity which wraps around the leading edge and forms streamwise vortices above the boundary layer. A small, but finite amplitude inhomogeneity considered in [15] leads to nonlinear motion in an inviscid region above the boundary layer, which excites localized flow separation.

In the present work the interaction of a flow non-uniformity with the blunt nose of a plate is considered under quite different assumptions about size and amplitude of disturbances. We focus on the linear evolution of infinitesimally small disturbances far downstream of the leading edge, where transient growth of disturbances takes place.

2. Problem formulation

Consider the flow of a viscous incompressible fluid over a blunt nose flat plate with leading edge of dimension $O(b')$ (see *figure 1*). The Cartesian coordinate system x', y', z' is introduced, where the x' coordinate is assumed to be in the streamwise direction with the origin at the leading edge, y' is in the spanwise direction, and z' measures the normal distance from the plate's surface. The upstream flow is assumed to be unidirectional and nominally uniform, except for a small $O(\varepsilon)$ steady spanwise periodic perturbation in the streamwise velocity. The streamwise velocity component far upstream is specified by:

$$u' = u_\infty\left(1 + \varepsilon \mathrm{e}^{-\sigma x'} \cos 2\pi y'/\lambda'\right), \tag{1}$$

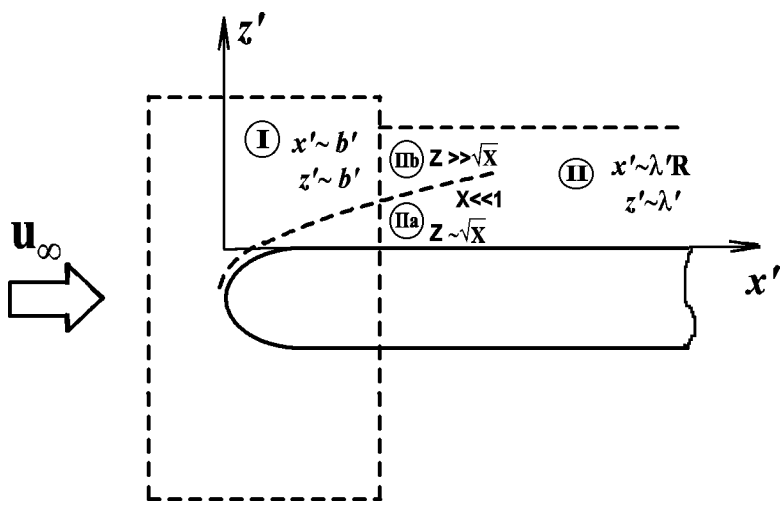

Figure 1. Schematic division of the flow field into regions.

where λ' is the spanwise period and $\sigma = 4\pi^2\nu/u_\infty\lambda'^2$. Further, we suppose that the Reynolds number $R = u_\infty\lambda'/\nu$ is large, so upstream flow (1) with zero vertical v' and spanwise w' velocity components is the solution of Navier–Stokes equations up to $O(\varepsilon/R)$ terms. Finally, we require that the period of the non-uniformity λ' be small with respect to nose size b'.

A linear (in ε) solution for distortion of boundary layer at the plate produced by upstream flow inhomogeneity will be sought. Hence, velocity components and pressure are linearized near flow around the plate in homogeneous stream as

$$u' = u_\infty\left[U_b(x', z') + \varepsilon u(x', z')\cos\frac{2\pi}{\lambda'}y'\right],$$

$$v' = u_\infty\left[\varepsilon v(x', z')\sin\frac{2\pi}{\lambda'}y'\right],$$

$$w' = u_\infty\left[W_b(x', z') + \varepsilon w(x', z')\cos\frac{2\pi}{\lambda'}y'\right],$$

$$p' = \rho u_\infty^2\left[P_b(x', z') + \varepsilon u(x', z')\cos\frac{2\pi}{\lambda'}y'\right].$$

Here U_b, W_b, P_b describe the two-dimensional basic flow, and u, v, w, p are perturbations of velocity and pressure excited by flow non-uniformity. The perturbations are governed by linearized Navier–Stokes equations with no-slip conditions at the plate and upstream conditions followed from (1)

$$u \to e^{-\sigma x'}, \quad v, w \to 0; \qquad x' \to -\infty. \tag{2}$$

3. Solution for $x'/\lambda' \ll R$

Matched asymptotic expansions method is applied to the problem under consideration and flow field is divided into two regions shown in *figure 1*. In the vicinity of the leading edge where $x', y' \sim b'$ (region I in *figure 1*) the flow is inviscid outside a thin boundary layer. The perturbations here are governed by linearized Euler equations with normal to the wall velocity vanishing at the wall. Due to small size of region I, the decay of disturbances in downstream direction caused by viscosity may be neglected, and upstream boundary conditions become

$$u \to 1, \quad v, w \to 0; \qquad x'/b' \to -\infty.$$

A similar problem about non-uniform flow near the leading edge was solved in [15]. There, it was found that far downstream the cross-flow velocity component becomes singular near the wall as

$$v \simeq -\frac{2\pi}{a}\left(\frac{b'}{\lambda'}\right)\ln\left(\frac{z'}{b'}\right); \quad z'/b' \to 0,\ x'/b' \to \infty, \tag{3}$$

where a is a constant related to the local potential flow behavior in the vicinity of the stagnation point. The remaining velocity components remain finite as

$$u \simeq 1, \qquad w \simeq -\frac{4\pi^2}{a}\left(\frac{b'}{\lambda'}\right)^2\frac{z'}{b'}\ln\left(\frac{z'}{b'}\right); \quad z'/b' \to 0,\ x'/b' \to \infty. \tag{4}$$

Viscous effects become significant further downstream in region II, whose length is $\sim \lambda' R$. The thickness of this region is defined by the vertical length of disturbances relaxation which is $\sim \lambda'$. In region II we introduce the non-dimensional variables $X = x'/\lambda' R$, $Z = z'/\lambda'$. For $X \ll 1$ this region may be divided into 'boundary layer' where $Z \sim \sqrt{X}$ (subregion IIa in *figure 1)* and an inviscid part (subregion IIb) where $Z \sim 1$. The upstream boundary conditions in the inviscid part of region II follow from the downstream limit of the solution in the vicinity of the leading edge (4)

$$u(0, z) = 1, \qquad v(0, z) = A, \qquad w(0, z) = -2\pi A Z. \tag{5}$$

Here $A = (2\pi b'/\lambda' a) \ln(b'/\lambda') \gg 1$.

The viscous part of region II is a continuation of the boundary layer of region I; hence upstream boundary conditions here should be found from the solution in this boundary layer. However, initial conditions in thin subregion IIb affect the flow only over a short initial portion of region II and the perturbations caused by these conditions are O(1), whereas the effect of initial conditions in outer subregion IIb spreads over a distance $x' \sim R\lambda'$ and manifests itself by excitation of streamwise velocity perturbation $\sim AR$. Hence, the effect of initial state of 'boundary layer' will be neglected and some solution here which is 'fitted' with the solution in the inviscid part will be used as initial condition for subregion IIb. A similar assumption, in fact, was made previously by Crow [14], and Goldstein et al. [15].

Due to the linearity of the problem under consideration, its solution may be presented as a sum of the solutions to two problems. The first problem deals with non-zero initial conditions for streamwise velocity and homogeneous conditions for cross-flow velocity. Its solution may be shown to be O(1) for all X. The second problem with non-zero initial conditions for cross-flow velocity and zero conditions for u is more interesting, because its solution describes transient growth of streamwise velocity perturbation to the value of $\sim AR$. Furthermore, we shall focus on the last problem solution, so we shall put $u(0, Z) = 0$ in initial conditions (5). The solution will be sought in the form

$$u = ARU(X, Z), \qquad v = AV(X, Z), \qquad w = AW(X, Z), \qquad p = \frac{A}{R} P(X, Z), \tag{6}$$

where normalized disturbances of velocity components and pressure U, V, W, P are universal functions of X, Z only, i.e. they are independent from any dimensional parameters and shape of leading edge. Substituting (6) into Navier–Stokes equations linearized near the Blasius basic flow

$$U_b = U_0(\eta), \qquad W_b = \frac{1}{R} W_0(\eta), \qquad P_b = \mathrm{O}\left(\frac{1}{R^2}\right),$$

$$U_0 = f', \qquad W_0 = \frac{1}{2\sqrt{X}}(\eta f' - f), \qquad \eta = z' \sqrt{\frac{u_\infty}{\nu x'}} = Z/\sqrt{X},$$

$$f''' + \frac{1}{2} f f'' = 0, \qquad f(0) = f'(0) = 0, \qquad f'(\infty) = 1,$$

and neglecting terms $O(1/R^2)$ the following set of equations for universal functions U, V, W, P is obtained

$$\begin{aligned}
&U_0\frac{\partial U}{\partial X}+\frac{\partial U_0}{\partial X}U+W_0\frac{\partial U}{\partial Z}+\frac{\partial U_0}{\partial Z}W=\frac{\partial^2 U}{\partial Z^2}-4\pi^2 U,\\
&U_0\frac{\partial V}{\partial X}+W_0\frac{\partial V}{\partial Z}=-2\pi P+\frac{\partial^2 V}{\partial Z^2}-4\pi^2 V,\\
&U_0\frac{\partial W}{\partial X}+\frac{\partial W_0}{\partial X}U+W_0\frac{\partial W}{\partial Z}+\frac{\partial W_0}{\partial Z}W=-\frac{\partial P}{\partial Z}+\frac{\partial^2 W}{\partial Z^2}-4\pi^2 W,\\
&\frac{\partial U}{\partial X}+2\pi V+\frac{\partial W}{\partial Z}=0.
\end{aligned}\tag{7}$$

These equations correspond exactly to the Goertler equations (with $\beta=2\pi$), with Goertler number zero, as introduced by Floryan and Saric [16] and Hall [17]. The same scaling of disturbances and equations were used by Andersson et al. [7] and Luchini [8] for study of optimal growth of disturbances in flat-plate boundary layer.

First, let us find the solution of (7) in subregion IIb where $Z\gg\sqrt{X}$ and the basic flow reduces to

$$U_0=1,\qquad W_0=W_{00}/\sqrt{X},\qquad W_{00}=\frac{1}{2}\lim_{\eta\to\infty}(\eta f'-f).$$

Initial conditions in this subregion follow from (5)

$$U(0,Z)=0,\qquad V(0,Z)=1,\qquad W(0,Z)=-2\pi Z \tag{8}$$

and boundary conditions for $Z\to 0$ should be found from matching with solution in subregion IIa. Putting $U\equiv 0$ and eliminating pressure from (7) we obtain a simple equation for W

$$\frac{\partial B}{\partial X}+\frac{W_{00}}{\sqrt{X}}\frac{\partial B}{\partial Z}=\frac{\partial^2 B}{\partial Z^2}-4\pi^2 B,\quad B=\frac{\partial^2 W}{\partial Z^2}-4\pi^2 W.$$

Its solution, which satisfies the initial conditions (8) and the boundary condition at the wall $W(X,0)=G(X)$ (G is arbitrary function), is

$$W=G(X)\mathrm{e}^{-2\pi Z}-2\pi\left(Z-2W_{00}\sqrt{X}\right)\mathrm{e}^{-4\pi^2 X}. \tag{9}$$

The spanwise velocity and pressure corresponding to this solution are

$$V=-G(X)\mathrm{e}^{-2\pi Z}+\mathrm{e}^{-4\pi^2 X};\qquad P=\left(-\frac{1}{2\pi}\frac{\mathrm{d}G}{\mathrm{d}X}+\frac{W_{00}}{\sqrt{X}}\right)\mathrm{e}^{-2\pi Z}. \tag{10}$$

It should be mentioned that the function $G(X)$ must vanish for $X\to 0$ in order to satisfy the initial conditions (8). The solution obtained provides the boundary conditions at the upper boundary of subregion IIa

$$U\to 0,\qquad V\to 1,\qquad W\to -2\pi Z;\qquad Z/\sqrt{X}\to\infty,\qquad X\ll 1.$$

The solution in initial part of boundary layer for the same boundary conditions was found by Crow [14]. In variables introduced here this solution takes form

$$\begin{aligned} U &= -\pi X \eta f'' + \mathrm{O}(X^{3/2}), \\ V &= f' + \mathrm{O}(X^{1/2}), \\ W &= \frac{\pi}{2}\sqrt{X}\left(-\eta^2 f'' + 3\eta f - 7f\right) + \mathrm{O}(X), \\ P &= \mathrm{O}(1/\sqrt{X}). \end{aligned} \tag{11}$$

4. Solution for $x'/\lambda' \sim R$

In the main part of region II where $X \sim 1$ the set of equations (7) are solved numerically. These equations are parabolic in X, and thus require initial conditions at some section $X = X_0$ and boundary conditions at the wall and $Z \to \infty$. Initial conditions are set at small X_0 using Crow solution (11). Boundary conditions for $Z \to \infty$ are obtained from the similar limit of solution in subregion IIb (9), (10) which remains valid for $X \sim 1$ when $Z \gg \sqrt{X}$.

$$U(X, Z) \to 0; \qquad V(X, Z) \to \mathrm{e}^{-4\pi^2 X}; \qquad W(X, Z) \to -2\pi\left(Z - 2W_{00}\sqrt{X}\right)\mathrm{e}^{-4\pi^2 X}; \qquad Z \to \infty.$$

The disturbance velocities are specified to be zero at the wall.

Equations (7) are solved by a marching procedure. The streamwise derivatives are approximated with an upwind second-order finite-difference scheme. In the wall-normal direction the spectral collocation formulation based on Laguerre polynomials is used to discretize these equations. The no-slip conditions at the wall are satisfied by means of proper choice of base functions. The boundary conditions at $Z \to \infty$ are set at a large, but finite distance from the wall $Z = Z_{\max} = 10$. This numerical method is similar to that used by Ustinov [18] for computations of laminar-turbulent transitions by PSE- method.

The solution was found to be independent from the location of the initial section X_0 (within an accuracy of $\sim 0.1\%$) when $X_0 \leqslant 10^{-5}$. *Figures 2* and *3* show the solution for U obtained under this condition. Other velocity components v and w of disturbance practically vanish compared to the u component for $X \geqslant 10^{-3}$, so they are not considered further. The maximal value over Z of the normalized streamwise velocity perturbation U_m as function of X is plotted in *figure 2* together with similar results for the asymptotic solution by Crow. For X less then 10^{-3} the numerical solution nearly coincides with asymptotic one and disturbances grow almost linearly. Furthermore, the amplitude of the disturbance reaches maximum at $X \simeq 0.02$ and then decays due to viscous dissipation. A similar behavior of disturbances generated by streamwise vortices in boundary layer was found in [7,8]. Vertical profiles of U at different distances from leading edge X are shown in *figure 3*. The maximum of these profiles gradually shifts outside from wall as X increases. However, before the disturbance reaches a maximum in X, its vertical profile nearly coincide with Crow's solution, shown by dashed line in *figure 3* and with profile of r.m.s. velocity perturbations measured in boundary layer subjected to free-stream turbulence by Westin et al. [2]. The shift of maximum with X becomes remarkable only for large distances, where the disturbance decays.

To show how the general parameters appear in the solution for u, let us rewrite (6) in dimensional variables

$$u(x) = \frac{2\pi}{a} R_b \ln\left(\frac{b'}{\lambda'}\right) U\left(\left(\frac{\delta'}{\lambda'}\right)^2, \frac{z'}{\lambda'}\right). \tag{12}$$

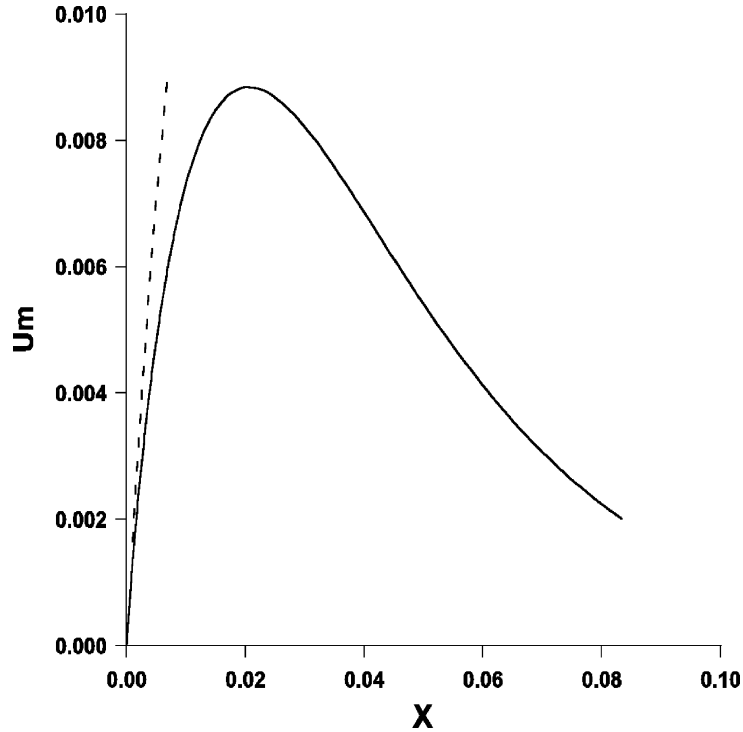

Figure 2. Maximal in Z normalized disturbances of streamwise velocity U as function of X. (———) – numerical solution, (- - - -) – Crow solution.

Here $\delta' = \sqrt{\nu x'/u_\infty}$ is the boundary layer thickness at the position where the disturbance is determined and $R_b = u_\infty b'/\nu$ is the Reynolds number computed using the size of nose bluntness b'. From (12) it follows that the maximal value reached by the disturbance in boundary layer u_m is proportional to R_b and only weakly (logarithmically) depends on the spanwise period λ'. This conclusion may be expressed by the simple relationship

$$u_m \simeq 0.055\frac{1}{a}R_b \ln\left(\frac{b'}{\lambda'}\right). \tag{13}$$

The downstream position x'_m giving the largest disturbance amplification is proportional to the square of its spanwise period λ' as

$$x'_m \simeq 0.02\frac{u_\infty}{\nu}\lambda'^2. \tag{14}$$

Another important conclusion from (12) is that the spanwise period λ'_m which gives the maximal amplification of the disturbance at a fixed downstream position x' is almost proportional to the boundary layer thickness at this position, i.e.

$$\lambda'_m \simeq 7.07\delta'\left(1 + \mathrm{O}\left(\ln\left(\frac{b'}{\lambda'}\right)\right)\right). \tag{15}$$

Relationships similar to (14) and (15) (with different coefficients) were found in [7,8] for disturbances exhibiting optimal energy growth in the boundary layer over an infinitely thin plate. Downstream growth of spanwise scale of boundary layer disturbances also have been observed in experiment [1,2]; however, this

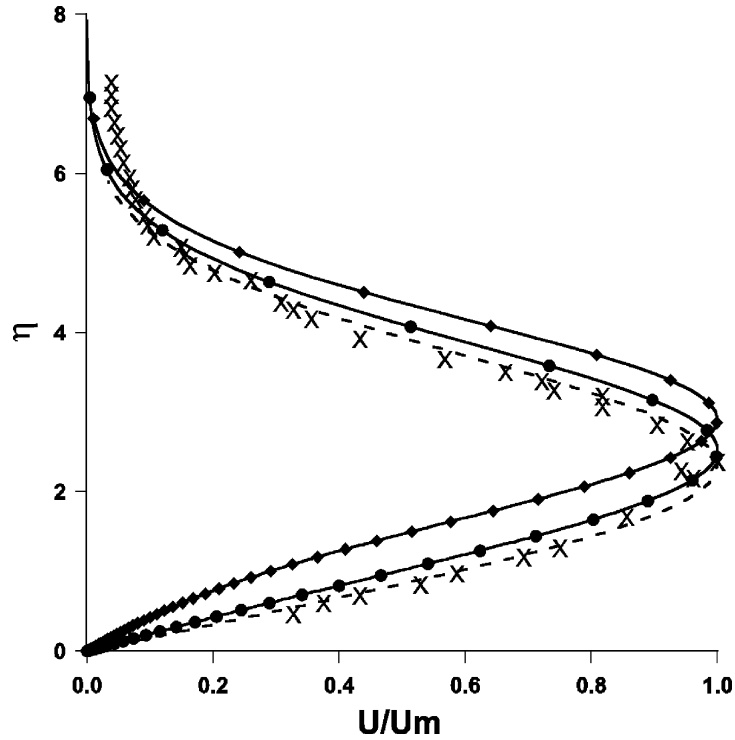

Figure 3. Vertical profiles of streamwise velocity disturbance. Solid lines correspond to numerical solution at $X = 0.02$ (—•—) and $X = 0.08$ (–♦–). Dashed line shows Crow solution. Points × – low-frequency pulsations in boundary layer subjected to free-stream turbulence [2].

growth is slower then the thickening of boundary layer. Disagreement with (15) and a similar conclusion drawn in [7,8] may be caused by the non-uniformity of spanwise wavenumber spectrum of oncoming turbulence in experiment.

However, the first conclusion about equal amplification of disturbances of all scales in boundary layer at blunt nose plate is in contradiction with all experimental and theoretical results obtained for plates with sharp leading edge. Theory [7,8] predicts, instead of (13) that $u_m \sim R = u_\infty \lambda'/\nu$. A similar conclusion may be derived from experiment of Westin et al. [2] if the amplitude growth data $u_m \sim \sqrt{R_x} = \sqrt{u_\infty x'/\nu}$ is considered together with correlation for spanwise period of pulsations $\lambda' \sim \delta' \sim \sqrt{\nu x'/u_\infty}$. The cause of such obvious disagreement is the additional amplification of disturbances caused by vorticity field deformation near the blunt leading edge. The amplification of disturbances in the latter case is accounted for by the coefficient A in (5), which is roughly inversely proportional to the spanwise period λ'. Further growth of disturbances in boundary layer occurs in accordance with theory [7,8] and experiment, and the amplification coefficient here is $\sim R$, i.e. proportional to λ'. Full amplification is a product of these two coefficients, so it is almost independent of the spanwise period.

The solution found reveals that the boundary layer developing over blunt bodies is more receptive to outer flow vortical disturbances than the one over a flat plate with a sharp leading edge (approximately by a factor b'/λ'). So, in flow with enhanced turbulence level, the transition Reynolds number for blunt bodies should be much smaller than that observed in well-known experiments [1–3] performed with sharp leading edge plates. Moreover, the scenario of transition over blunt bodies may be quite different, due to the different dependence of disturbances' amplification from their spanwise scale.

5. Boundary layer response to a localized flow non-uniformity

Based on the solution for periodic outer flow inhomogeneity the response of boundary layer at the blunt nosed plate is now searched for the localized flow non-uniformity. We assume that its profile is given by a function $g(y)$, expressible as a Fourier integral, so we shall consider inflow conditions of form

$$u(x', y', z') = u_\infty\big(1 + \varepsilon g(y)\big), \quad v',\ w' = 0;\ x'/b' \to -\infty,\ g(y) = \int_{-\infty}^{\infty} F(\beta)\mathrm{e}^{i\beta y}\,\mathrm{d}\beta. \tag{16}$$

Here $y = y'/d'$ is the non-dimensional spanwise coordinate introduced using the characteristic width of inhomogeneity d' and $F(\beta)$ is Fourier transform of $g(y)$. As for periodic non-uniformity, the characteristic width d' is assumed to be small with respect to the size of nose bluntness. A linear solution for disturbances in boundary layer is sought, and the streamwise velocity component is presented in the form

$$u'(x', y, z') = u_\infty\big(U_0(\eta) + \varepsilon u(x', y, z')\big); \quad x'/d' \gg 1,$$

where $U_0(\eta)$ is the basic flow with Blasius velocity profile, u is perturbation of streamwise velocity. Due to linearity of the problem the solution for u may be found as a Fourier integral:

$$u(x', y, z') = \int_{-\infty}^{+\infty} F(\beta)\widehat{u}(x', \beta, z')\mathrm{e}^{i\beta y}\,\mathrm{d}\beta, \tag{17}$$

where $\widehat{u}(x', \beta, z')\mathrm{e}^{i\beta y}$ is the perturbation produced by periodic non-uniformity of unit amplitude with profile $g_1(y) = \mathrm{e}^{i\beta y}$. The amplitude of the last perturbation $\widehat{u}(x', \beta, z')$ is readily derived from (12) by substituting $2\pi d'/\beta$ for λ'.

$$\widehat{u}(x', \beta, z') = \frac{2\pi}{a} R_b \ln\left(\frac{b'\beta}{2\pi d'}\right) U\left(\frac{\beta^2}{4\pi^2}\frac{\nu x'}{u_\infty d^2}, \frac{\beta}{2\pi}\frac{z'}{d'}\right).$$

Substituting this into (17) and neglecting $\mathrm{O}(\ln\beta)$ term as small compared with $\ln(\frac{b'}{2\pi d'})$, the following solution for perturbation from localized non-uniformity is obtained

$$u = \overline{A}\, R_b\, \overline{U}(\overline{X}, y, \overline{Z}), \quad \overline{U}(\overline{X}, y, \overline{Z}) = \int_{-\infty}^{+\infty} F(\beta) U\big(\beta^2\overline{X}, \beta\overline{Z}\big)\mathrm{e}^{i\beta y}\,\mathrm{d}\beta. \tag{18}$$

Here $\overline{X} = \frac{\nu x'}{4\pi^2 u_\infty d'^2}$, $\overline{Z} = \frac{z'}{2\pi d'}$, $\overline{A} = \frac{2\pi}{a}\ln(b'/2\pi d')$, and the function U in the integral is the universal solution for periodic outer flow non-uniformity found in the previous section. The first expression in (18) reflects the dependence of the solution on basic parameters. The second one defines the normalized perturbation of streamwise velocity $\overline{U}$ which is determined by oncoming non-uniformity profile $g(y)$ solely, and is independent from any dimensional values. Near the nose, where $\overline{X} \ll 1$, Crow's solution for U (11) is valid and the second expression in (18) reduces to

$$\overline{U}(\overline{X}, y, \overline{Z}) \simeq \pi\overline{X}\eta f''(\eta)\frac{\mathrm{d}^2 g}{\mathrm{d}y^2}; \quad \overline{X} \ll 1. \tag{19}$$

This simple asymptotic solution shows that if the oncoming non-uniformity is not sinusoidal, the velocity perturbation profile in the boundary layer is quite different from the oncoming profile.

As an example, let us consider the boundary layer response to a flow non-uniformity produced by a laminar wake behind a cylinder placed normal to the leading edge. Its profile is given by the Gaussian distribution:

$$g(y) = -\mathrm{e}^{-y^2}.$$

Normalized perturbation of streamwise velocity $\overline{U}$ for this profile computed using (18) from universal solution $U(X)$ is shown by solid lines in *figures 4* and *5*. *Figure 4* shows its maximum in (y, z) plane $\overline{U}_m$ as a function of $\overline{X}$. Unlike the similar curve for sinusoidal non-uniformity, the perturbation produced by the wake decays very slowly after it reaches its maximum. Spanwise profiles of normalized disturbance in boundary layer at vertical distance from wall $z' = 2.2\delta'$ for different non-dimensional distances from leading edge $\overline{X}$ are plotted in *figure 5*. These profiles have two maximums on sides of minimum at $y = 0$ and are quite different from oncoming profile. The disturbance in boundary layer spreads gradually in the spanwise direction during its streamwise evolution. At $\overline{X} = 0.008$ where the disturbance reaches its maximum in $\overline{X}$, its profile is 1.5 times wider and at $\overline{X} = 0.02$ it is 2 times wider then those near the leading edge. Unlike spanwise profile of disturbance, its vertical profile remains almost the same before maximum in $\overline{X}$ and is well described by Crow's solution.

Dashed lines in *figures 4* and *5* show asymptotic solution (19). It gives linear growth of perturbations and coincides well with the exact one (18) at small distances $\overline{X} \leqslant 0.001$ only. For larger $\overline{X}$ the asymptotic solution gives incorrect amplitude of disturbance as well as incorrect shape of its spanwise profile. However this solution is useful enough to explain the transformation of oncoming non-uniformity profile into a quite different profile of perturbation in the initial part of the boundary layer. Subsequent spreading of this profile is readily related with properties of the solution for the periodic non-uniformity. When $\overline{X}$ is small, all harmonics exhibit linear growth in $\overline{X}$. The linear growth of all harmonics (with different growth rates proportional to β^2) results in the

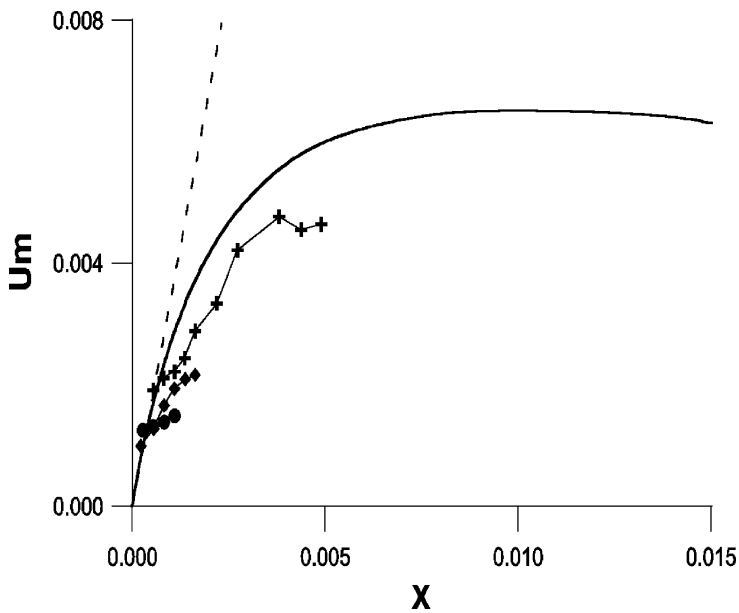

Figure 4. Maximal in normal to flow plane normalized disturbance $\overline{U}$ produced by Gaussian profile flow non-uniformity. (——) – numerical solution; (- - - -) – asymptotic solution (19). Experimental data [19] for plates with semi-elliptic noses of aspect ratious 1:8 – (—+—); 1:4 – (—♦—); 1:2 – (—•—).

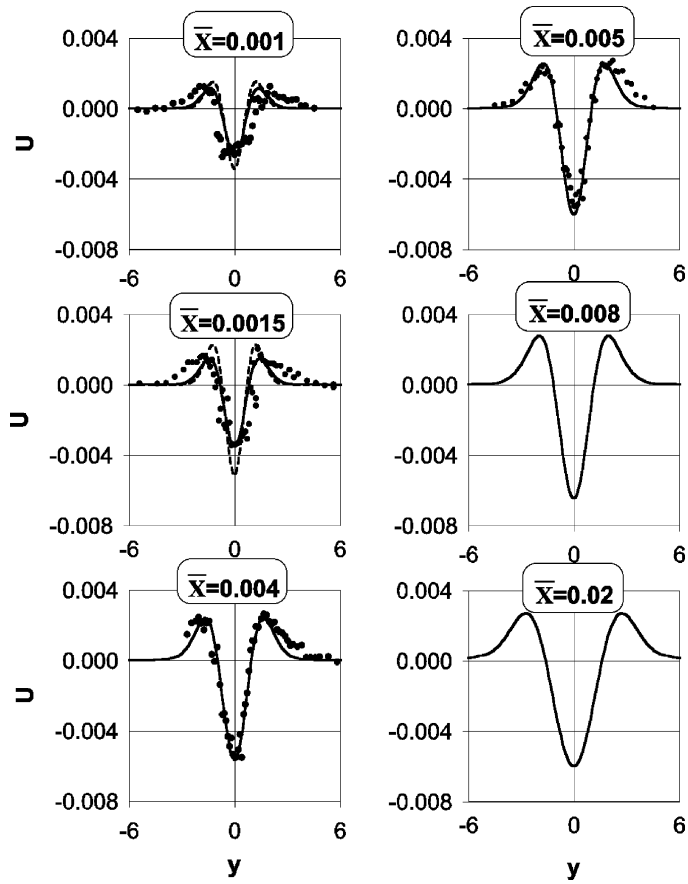

Figure 5. Spanwise profiles of disturbance produced by gaussian profile non-uniformity at different streamwise positions. (——) – numerical solution; (- - -) – asymptotic solution; points • – experimental data [19] for 1:8 nose plate.

self-similar profile given by (19). For larger $\overline{X}$ the growth of high-β harmonics saturates (at $\overline{X} \sim 1/\beta^2$), and the contribution of large-period components in Fourier integral increases, so the profile gradually becomes wider.

The solution for a Gaussian profile of the inhomogeneity permits a direct comparison with the experiment of Ustinov et al. [19], where the interaction of the wake behind a wire stretched normal to leading edge with the boundary layer at the blunt nose plate was studied. Different combinations of wire diameter, distance from wire to leading edge, flow velocity, and shapes of the plate's nose were tested in [19]. However, for comparison with theory we chose only the results obtained for wire diameter 0.09 mm, flow velocity $u_\infty = 17$ m/s and maximal distance from wire to leading edge $L = 720$ mm, for, in this case only, the oncoming flow non-uniformity was small enough to consider the wake/boundary layer interaction as linear. For these parameters, the non-uniformity had amplitude $\varepsilon = 0.02$ and width $d' \simeq 1.7$ mm. Interaction of this wake with a boundary layer at three plates of thickness (or characteristic size of nose) $b' = 2$ sm and semi-elliptic noses of aspect ratious $1:8$, $1:4$ and $1:2$ was studied. The data in form of maximal perturbation of streamwise velocity in boundary layer u'_m as function of streamwise coordinate x' were obtained. To compare with theory, the value similar to maximum of normalized disturbance $\overline{U}_m$ was computed from these data as

$$\overline{U}_m = \frac{u'_m}{\pi \varepsilon u_\infty R_r \ln(b'/2\pi d')}. \tag{20}$$

Here $R_r = u_\infty r'/\nu$; r' is the radius of leading edge. To derive this formula the relationship $a = 2b'/r'$ valid for all bodies with blunt leading edge was used. The curves $\overline{U}_m$ versus $\overline{X}$ computed from experimental data for all three plates are plotted in *figure 4* together with similar theoretical curve. Comparison with experiment shows that theory overestimates amplification of disturbances approximately 1.2 times. This disagreement is not dramatic because the logarithmic term which in (19) was assumed to be large, was O(1) in experiment.

Spanwise profiles of velocity in boundary layer measured at plate with 1 : 8 nose at sections $x' = 0.2, 0.3, 0.7, 0.9$ m (corresponding to $\overline{X} = 0.00109,\ 0.00163,\ 0.00381,\ 0.0049$ respectively) are plotted in *figure 5* together with similar results from the theory. For convenience, the experimental results were normalized by multiplying by some coefficient (equal for all sections) to achieve the best coincidence with theoretical profiles. *Figure 5* demonstrates that the exact solution (18) predicts well the shapes of spanwise profiles in boundary layer as well as their relative amplitudes.

6. Conclusions

The response of a boundary layer developing over the flat plate with blunt nose to infinitesimally small non-uniformities in the freestream velocity was studied. It was shown that oncoming spanwise periodic non-uniformities excite boundary layer disturbances similar to streaks, or Klebanoff modes, generally observed in experiments conducted with enhanced free-stream turbulence level. These disturbances have predominantly streamwise velocity component and exhibit transient growth. The solution obtained appears in the form of a similarity law, so that its dependence on all parameters is highlighted. The largest amplification of disturbances was shown to be proportional to the Reynolds number based on the size of nose bluntness and almost independent on the spanwise period. This surprising property is caused by additional amplification of disturbances via vortex lines stretching around leading edge, an effect discovered by Goldstein et al. [15].

It was also found that the spanwise profile of boundary layer flow inhomogeneity is different from that of the oncoming flow. Near the leading edge (for $\overline{X} \ll 1$) it is proportional to the second derivative of oncoming flow profile with respect to spanwise coordinate. Comparison of results obtained here with experiment of Ustinov et al. [19] dealing with wake/flat plate boundary layer interaction show good coincidence of spanwise profiles of boundary layer disturbances and their relative amplitudes.

In general, it was found that the shape of the leading edge drastically affects the receptivity of the boundary layer to vortical disturbances.

Acknowledgments

The research was made with financial support of Russian Foundation of Fundamental Researches (Grant #98-01-00626).

References

[1] Kendall J.M., Boundary layer receptivity to free stream turbulence, AIAA Paper 90-1504, 1990.
[2] Westin K.J.A., Boiko A.V., Klingmann B.G.B., Kozlov V.V., Alfredsson P.H., Experiments in a boundary layer subjected to free stream turbulence. Part I: Boundary layer structure and receptivity, J. Fluid Mech. 221 (1994) 193–218.
[3] Alfredsson P.H., Matsubara M., Streaky structures in transition, in: Henkes R.A.W.M., van Ingen J.L. (Eds.), Trasitional Boundary Layers in Aeronautics, Elsevier, 1996.
[4] Morkovin M.V., The many faces of transition, in: Wells C.S. (Ed.), Viscous Drag Reduction, Plenum Press, 1969.
[5] Herbert T., Lin M.L., Studies of boundary-layer receptivity with parabolized stability equations, AIAA Paper 93-3053, 1993.

[6] Bertolotti F.P., Response of the Blasius boundary layer to free-stream vorticity, Phys. Fluids 9 (1997) 2286–2299.
[7] Andersson P., Berggren M., Henningson D.S., Optimal disturbances and bypass transition in boundary layers, Phys. Fluids 11 (1999) 134–150.
[8] Luchini P., Reynolds-number-independent instability of the boundary layer over a flat surface: optimal perturbations, J. Fluid Mech. 404 (2000) 289–309.
[9] Reshotko E., Tumin A., Optimal spatial disturbances in circular pipe flow, Abstract Book, 20th International Congress of Theoretical and Applied Mechanics, p. 19.
[10] Bradshaw P., The effect of wind-tunnel screens on nominally two-dimensional boundary layers, J. Fluid Mech. 22 (1965) 679–687.
[11] Watmuff J.H., Detrimental effects of almost immeasurably small freestream nonuniformities generated by wing-tunnel screens, AIAA J. 36 (1998) 3–11.
[12] Kachanov Y.S., Kozlov V.V., Levchenko V.Y., Origin of Tollmien–Schlichting waves in boundary layer under the influence of external disturbances, Izv. Akad. Nauk SSSR, Mekh. Zhidk. Gaza 5 (1978) 85–94. Translated in English in: Fluid Dyn. 13 (1979) 704–715.
[13] Sboev D.S., Grek G.R., Kozlov V.V., Experimental study of boundary layer receptivity to localized outer-flow disturbances, Teplofizica i Aeromehanica 8 (1) (1999) 1–14 (in Russian).
[14] Crow S.C., The spanwise perturbations of two-dimensional boundary layers, J. Fluid Mech. 24 (1966) 153–164.
[15] Goldstein M.E., Leib S.J., Cowley S.J., Distortion of a flat-plate boundary layer by free-stream vorticity normal to the plate, J. Fluid Mech. 237 (1992) 231–260.
[16] Floryan J.M., Saric W.S., Stability of Goertler vortices in boundary layers with suction, AIAA Paper 79-1497, 1979.
[17] Hall P., The linear development of Goertler vortices in growing boundary layers, J. Fluid Mech. 130 (1983) 41–65.
[18] Ustinov M.V., Interaction of a Tollmien–Schlichting wave with a local flow inhomogeneity, J. Appl. Mech. Tech. Phys. 39 (1) (1998) 65–72.
[19] Ustinov M.V., Kogan M.N., Shumilkin V.G., Zhigulev S.G., Experimental study of flat-plate boundary layer receptivity to vorticity normal to leading edge, in: Laminar–Turbulent Transition, IUTAM Symposium, Sedona, Az., 1999, Springer-Verlag (to appear).